

SC5381 and IH–SC1785 – Rheo-echo-XPCS to study the dynamic of the yielding transition in colloidal glasses

George Petekidis,¹ Nikolaos Burger,¹ Stefano Aime,² Fabio Giavazzi,³ Phillippe Bourrienne,² Roberto Cerbino,⁴ William Chevremont,⁵ Narayanan Theyencheri,⁵ Eric Freyssingas,⁶ and Thomas Gibaud⁶

¹*Crete*

²*ESPCI*

³*Milan*

⁴*Vienna*

⁵*ESRF*

⁶*Univ Lyon, Ens de Lyon, Univ Claude Bernard,
CNRS, Laboratoire de Physique, F69342 Lyon, France*

(Dated: September 22, 2023)

Report on the run SC5381 and IH–SC1785 that took place at ID02 the 31/09/2023 and the 20/06/2023.

Please be aware that for the moment the authors order is quite arbitrary and will need to be discuss later on in the process.

PACS numbers: xxx

I. INTRODUCTION

The glass state is a disordered solid state obtained at very high volume fractions. The glass transition is a dynamical arrested transition where colloids are trapped within the cage formed by their neighbours [1,2]. The absence of rearrangement on long time scales leads to the solid behaviour of the suspension. The glassy suspension may yield and become fluid upon application of an oscillatory strain with an amplitude above the yield strain σ_y [3].

Here we aim to study the yielding transition induced by shear in two distinct colloidal glass suspensions one composed of hard sphere particles (ludox dispersed in water [4]) and of model hard spheres dispersion. We will follow the protocol proposed by [6,7] where they performed oscillatory strain experiments at constant strain amplitude and construct the particle displacements or the intermediate scattering function following measurement at exactly the oscillatory period imposed by the rheometer. These echo measurements enables us to sample the microscopic configuration and dynamic at each deformation cycle, based on stroboscopic movies. We have adapt this protocol on beamline ID02 coupling a rheometer and echo-XPCS measurements.

Experiments using confocal measurements on colloidal hard sphere glasses show growing clusters of nonaffine deformation percolating at yielding [8]. Echo-image correlation velocimetry performed with a light microscope on glassy emulsion corroborate those results and show that the shear-induced dynamics are very heterogenous: quiescent particles coexist with mobile particles and when the domain of mobile particle percolate the sample yield [9]. Finally Echo-differential dynamic microscopy measurements performed on traced in carbopol glass show that the shear-induced dynamics of the tracers is diffusive and heterogenous. This dynamic accelerate and

becomes homogeneous approaching σ_y [10].

Please find below a first draft of the analysis of the data. This is work in progress. There are still plenty of analysis to carry out.

II. MATERIALS AND METHODS

A. PMMA hard spheres

The colloidal particles in this study consist of poly(methylmethacrylate) (PMMA) spheres with an average radius of $R = 340$ nm. These spheres are sterically stabilized by a thin layer of poly(12-hydroxystearic) acid, which has a thickness of approximately 10 nm. These colloidal particles are similar in physical characteristics to those utilized in previous research on the glass transition (as seen in references [4, 11, 19]). These particles are intentionally polydisperse, with a standard deviation of approximately 10% in their size distribution. This polydispersity is designed to prevent crystallization for an extended period, lasting several months, which is significantly longer than the typical duration of experiments.

These colloidal particles are suspended in a mixture of cis/trans-decalin. This solvent has a refractive index of 1.48 at a temperature of $T = 25^\circ\text{C}$, which is slightly below the refractive index of the colloidal particles (1.5). This matching of refractive indices minimizes van der Waals attractions between the particles and allows for light scattering experiments to be conducted in the single scattering regime. In the present study we focus on the concentration $\phi = 60\%$.

As shown in the Fig 1a, The dispersion at in the glassy regime at $\phi = 60\%$ display the classical spectrum of a hard sphere system. Its dynamics measure with "classical" XPCS display two decorrelation times associated with the α and β relaxation (Fig 1b).

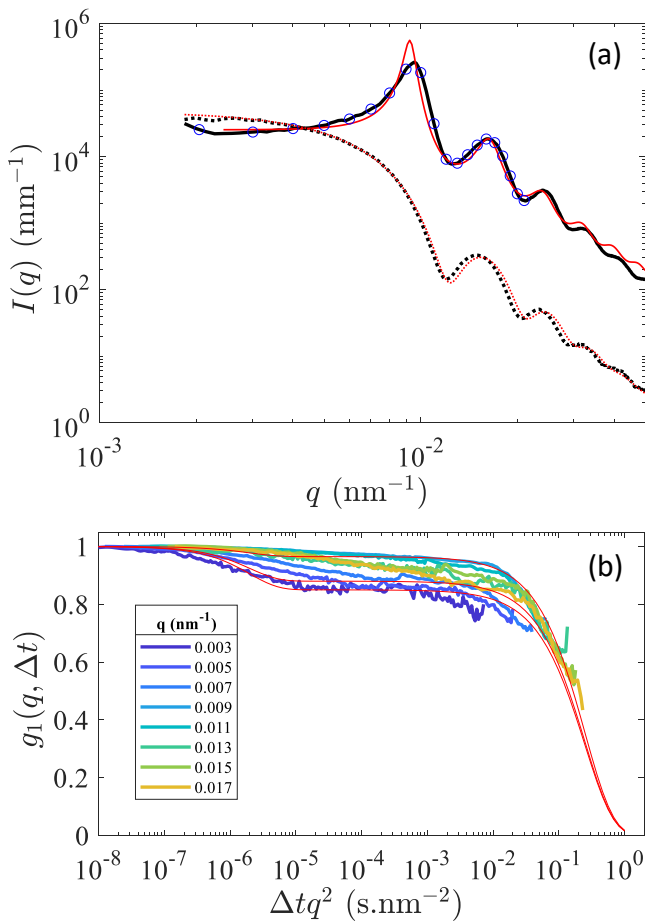


FIG. 1. Static and dynamics measurements of a suspension in quiescent conditions. (a) $I(q)$ at $\phi = 1\%$ (dash line) is the form factor. The form factor is fitted by a spherical core shell model with a shell of 10 nm and a core radius of $R = 340$ nm with a polydispersity of 9%. $I(q)$ at $\phi = 60\%$ (dash line) is fitted by hard sphere model [?]. blue circles indicate the q -values at which XPCS was carried out. (b) Autocorrelation function $g_1(q, \Delta t)$ of the glassy suspension at $\phi = 60\%$. Red lines are fits of the form $g_1 = (1 - f)e^{(-D_1 q^2 \Delta t)} + f e^{(-D_2 q^2 \Delta t)}$ with $D_1 = 510^5 \text{ nm}^2/\text{s}$ and $D_2 = 4 \text{ nm}^2/\text{s}$

B. Rheo-echo-XPCS protocol

The microstructural and dynamical properties of the fumed silica dispersion are investigated using XPCS and SAXS on the ID02 beamline at the European Synchrotron Radiation Facility (ESRF, Grenoble, France) [?].

The rheometer is set to oscillate at $f_0 = 0.1$ Hz and at a constant stress amplitude σ . We observe that after a few oscillations the elastic G' and loss modulus G'' become stationary. In this regime, we carry out rheo-echo-XPCS in bunch mode in the radial geometry. The bunch mode acquisition consists of 2000 2D spectra $I(q, t)$ acquired over time. This acquisition is divided into 20 groups, or "bunches," of rapid acquisitions. Each of these

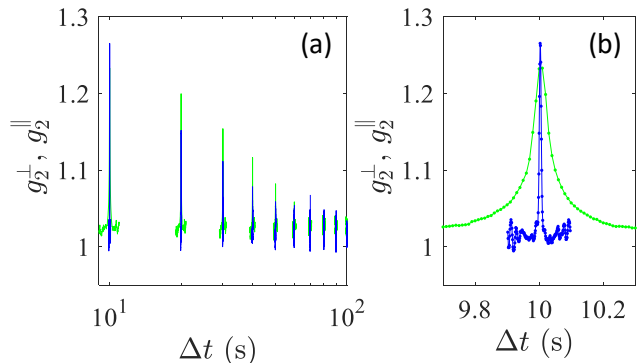


FIG. 2. Rheo-echo-XPCS. (a) g_2^{\parallel} (blue) and g_2^{\perp} (green) as a function of the lag time at $\sigma = 0.03$ Pa at $f_0 = 0.1$ Hz. (b) zoom on the first echo peak.

fast acquisitions is comprised of 100 spectra acquired at f_{bunch} . Furthermore, these fast acquisitions are repeated 20 times, with a frequency f_{echo} that is a sub-multiple of the oscillation frequency f_0 of the rheometer. Optimization of those frequencies have lead us to settled for $f_{echo} = f_0$ and $f_0/4$ and $f_{bunch} = 100$ Hz and 1 kHz.

Subsequently, the raw autocorrelation function $g_2(q, \Delta t)$ is calculated with respect to the lag time Δt and the wave vector q in two distinct directions: g_2^{\parallel} in the flow direction, along q_{\parallel} , and g_2^{\perp} in the vorticity direction, along q_{\perp} . In Fig. 2, as expected, we observe that g_2 exhibits peaks at time lags that align with multiples of $1/f_{echo}$. Notably, these peaks, referred to as "echo peaks," are much thinner in the vorticity direction compared to the flow direction. We also observe that the g_2^{\parallel} decorrelate faster than g_2^{\perp} .

III. RESULTS

To elucidate the underlying physics that govern the suspension dynamics under oscillatory shear, we proceed by monitoring both the amplitude and the time location of these peaks. This process enables us to reconstruct the autocorrelation function, as depicted in Figure 3. Importantly, we perform this analysis for various values of the wave vector q . In our preliminary scaling analysis of g_2 , we have uncovered distinctive behaviors:

- g_2^{\parallel} appears to follow a ballistic pattern, as g_2^{\parallel} measurements at different q values align when plotted as a function of $\Delta t q$.
- On the other hand, g_2^{\perp} exhibits a diffusive behavior, as g_2^{\perp} measurements at different q values superimpose when plotted as a function of $\Delta t q^2$. This allows us to extract a diffusion coefficient D_2^{\perp} by fitting the ensemble of scaled autocorrelation functions by $g_2 = 1 + \beta [e^{(-\Delta t q^2 D_2^{\perp})}]^2$.

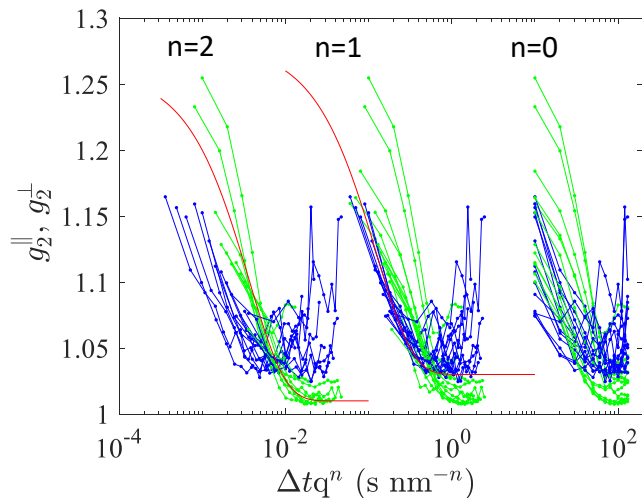


FIG. 3. Rheo-echo-XPCS. (a) g_2^{\parallel} (blue) and g_2^{\perp} (green) as a function of Δtq^n at $\sigma = 0.03$ Pa at $f_0 = 0.1$ Hz. $n = 0$ indicates unscaled data. $n = 1$ allows to probe a ballistic scaling. $n = 2$ allows to probe to a diffusive scaling.

We have conducted repeated experiments and analyses while varying the amplitude σ of the stress oscillations at $f_0 = 0.1$ Hz, and our results closely resemble those presented in Fig. 3. Finally, we have plotted the relative diffusive coefficient, D_2^{\perp} , as a function of the stress amplitude σ in Fig 4. We observe a significant increase in D_2^{\perp} as we approach σ_y , the onset of the fluidization. At rest ($\sigma = 0$ Pa), there are two measurements: the one measured in the capillary display a lower diffusion coefficient, as the sample has aged significantly, while, the one measured in the rheometer was rejuvenated, and is therefore

in agreement with the measurements at $\sigma \neq 0$ Pa.

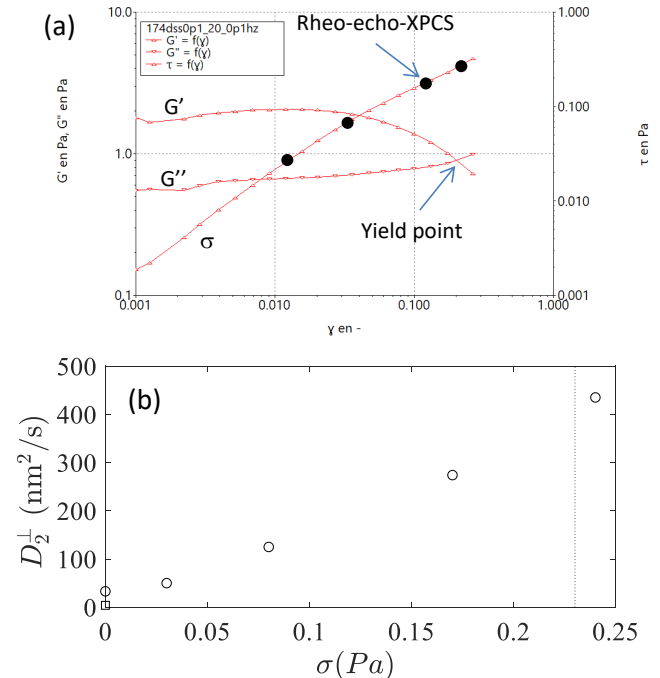


FIG. 4. Dynamics of the yielding transition. (a) stress sweep experiments carried out at $f_0 = 0.1$ Hz. Evolution of the elastic modulus G' , the loss modulus G'' and the stress σ as a function of the strain γ . Circles indicates where the rheo-echo-XPCS were carried out. (b) Diffusion coefficient in the vorticity direction D_2^{\perp} extracted from rheo-echo-XPCS measurement as a function of the stress amplitude σ at $f_0 = 0.1$ Hz. The square symbol indicate measurements in a capillary while circle symbols are measurements carried out in the rheometer. The vertical dash line represent the yield stress σ_y of the dispersion.